Nifontova *et al. Stem Cell Research & Therapy* (2024) 15:371
https://doi.org/10.1186/s13287-024-03976-x

Stem Cell Research & Therapy

REVIEW Open Access

Advancing wound healing by hydrogel-based dressings loaded with cell-conditioned medium: a systematic review

Galina Nifontova[1†], Sofia Safaryan[1†], Yana Khristidis[1], Olga Smirnova[1], Massoud Vosough[2], Anastasia Shpichka[1*] and Peter Timashev[1,3]

Abstract

Background Wound healing represents a complex biological process, critically important in clinical practice due to its direct implication in a patient's recovery and quality of life. Conservative wound management frequently falls short in providing an ideal environment for the optimal tissue regeneration, often resulting in extended healing periods and elevated risk of infection and other complications. The emerging biomaterials, particularly hydrogels, have shown substantial promise in addressing these challenges by offering properties such as biocompatibility, biodegradability, and the ability to cure wound environment. Recent advancements have highlighted the therapeutic potential of integrating cell-derived conditioned medium (CM) into hydrogel matrices. Cell-derived CM represents a rich array of bioactive molecules, demonstrating significant efficacy in modulating cellular activities crucial for wound healing, including cellular proliferation, migration, and angiogenesis.

Methods The methodology of this review adheres to the standards set by the Preferred Reporting Items for Systematic Review and Meta-Analysis (PRISMA) guidelines. The review includes a selection of studies published within the last five years, focusing on in vivo experiments involving various types of skin injuries treated with topically applied hydrogels loaded with CM (H-CM). The search strategy refers to the PICO framework and includes the assessment of study quality by CAMARADES tool.

Results The systematic review represents a detailed evaluation of H-CM dressings wound healing efficiency based on the experimental results of cell-based assays and animal wound models. The study targets to reveal wound healing capacity of H-CM dressings, and provides a comparative data analysis, limitations of methods and discussions of H-CM role in advancing the wound healing therapy.

Conclusions The data presented demonstrate that H-CM is a promising material for advanced wound healing and regenerative medicine. These dressings possess proved *in vitro/in vivo* efficacy that highlights their strong clinical potential and paves the way to further investigations of H-CM formulations within clinical trials.

[†]Galina Nifontova and Sofia Safaryan contributed equally to this work.

*Correspondence:
Anastasia Shpichka
ana-shpichka@yandex.ru

Full list of author information is available at the end of the article

Keywords Wound healing, Tissue regeneration, Dressings, Hydrogels, Crosslinking, Cell-conditioned medium, Proteome, Cell secretome, Animal models, In vitro/in vivo studies

Background

Wound healing is one of the most pressing challenges in modern regenerative medicine and tissue engineering due to its complexity and a high risk of chronification, especially when associated with diabetes [1–3]. The main stages of wound repair are hemostasis, inflammation, proliferation, and remodeling that are actively accompanied by immune events [4–8]. To provide the tissue repair and regeneration along with standard therapeutic strategies, novel biomaterials affecting biochemical, cellular and immunological processes have been recently introduced. These include self-pumping Janus-like dressings [9], microneedles [10], nanofibers [11], electrospun membranes [12, 13], and scaffolds [14, 15].

Hydrogels have emerged as effective materials for wound management and treatment enhancing tissue regeneration due to the composition of the hydrogel network [16]. The ability of the 3D-hydrogel network to retain moisture, its responsiveness to physical or chemical stimuli such as pH [17], temperature or light [18, 19], biocompatibility and biodegradability [20–22], oxygen-permeability [23, 24], bioadhesion [25, 26] ensure the delivery and controlled release of encapsulated active components in the target area. The active components may consist of antibiotic or anti-inflammatory drugs [27–29], nanoparticles [30, 31], therapeutic proteins, or nucleic acids [32–36]. Hydrogel-based dressings were demonstrated to modulate the macrophage response and polarization, thus enhancing angiogenesis in diabetic wounds [37, 38]. To facilitate immunostimulation and to induce cell proliferation, vascular endothelial or basic fibroblast growth factors were encapsulated into a hydrogel matrix [39, 40].

However, faster and more effective wound healing is expected in the case of a treatment based on cell secretome products rather than on single growth factors. This is related to the complexity of the wound microenvironment and biochemical cascades involved in tissue regeneration. Cell-derived conditioned medium (CM) represents a cell secretome containing extracellular vesicles and a large panel of biomolecules including mRNAs, active lipids, growth factors, growth-factor-binding proteins, cytokines, chemokines, and other biomolecules that enhance cell proliferation, migration, and angiogenesis [41–43]. It makes CM a cell-free alternative therapeutic comparing to the already existing mesenchymal stem cell-based wound treatments [44]. Hydrogels are ideal matrices preserving the structure and function of biomolecules, suitable for encapsulation of hydrophilic biomolecules such as proteins and nucleic acids. Tuning the hydrogel's mesh size, it is possible to control its mechanical strength and release rate of entrapped molecules. Thus, loading of a hydrogel matrix with CM represents a synergetic approach to promoting tissue regeneration, with the creation of a depot. The latter ensures prolonged release of CM components that finally improves the compliance of the wound treatment and management [45]. In this systematic review, we aim to analyze the wound healing efficiency of hydrogels loaded with CM (H-CM) engineered to be used as dressings (Fig. 1). Here, we target the design, approaches exploited for H-CM fabrication and *in vitro/in vivo* functionality assessment of such systems to reveal their wound healing capacity. We also consider the advantages and limitations of the designed methods, analyze the opportunities to use H-CM formulations as effective wound dressings, and discuss a possibility of further clinical studies of the resultant product.

Methods

The systematic review was conducted according to the guidelines of the Preferred Reporting Items for Systematic Review and Meta-Analysis (PRISMA) [46, 47]. The search was conducted via the PubMed and Scopus databases using the PICO process and involved the study quality assessment by the Collaborative Approach to Meta-Analysis and Review of Animal Data from Experimental Studies (CAMARADES). The systematic review was not pre-registered.

Research question

Is wound contraction in animal models due to the application of H-CM dressings more effective than treating wounds with CM or hydrogels alone?

Search strategy

The literature search was performed by the Boolean Operator using the "AND/OR" system and included all articles published within the last 5 years before March 2024. The following search query was used to collect relevant articles: ("conditioned" AND "medium" OR "secretome") AND ("hydrogel" OR "patch" OR "dressing") AND ("wound" OR "healing" OR "burn").

Study selection

Two reviewers (S.S. & G.N.) independently screened the titles and abstracts for all relevant studies to eliminate duplicates and select articles by eligibility criteria.

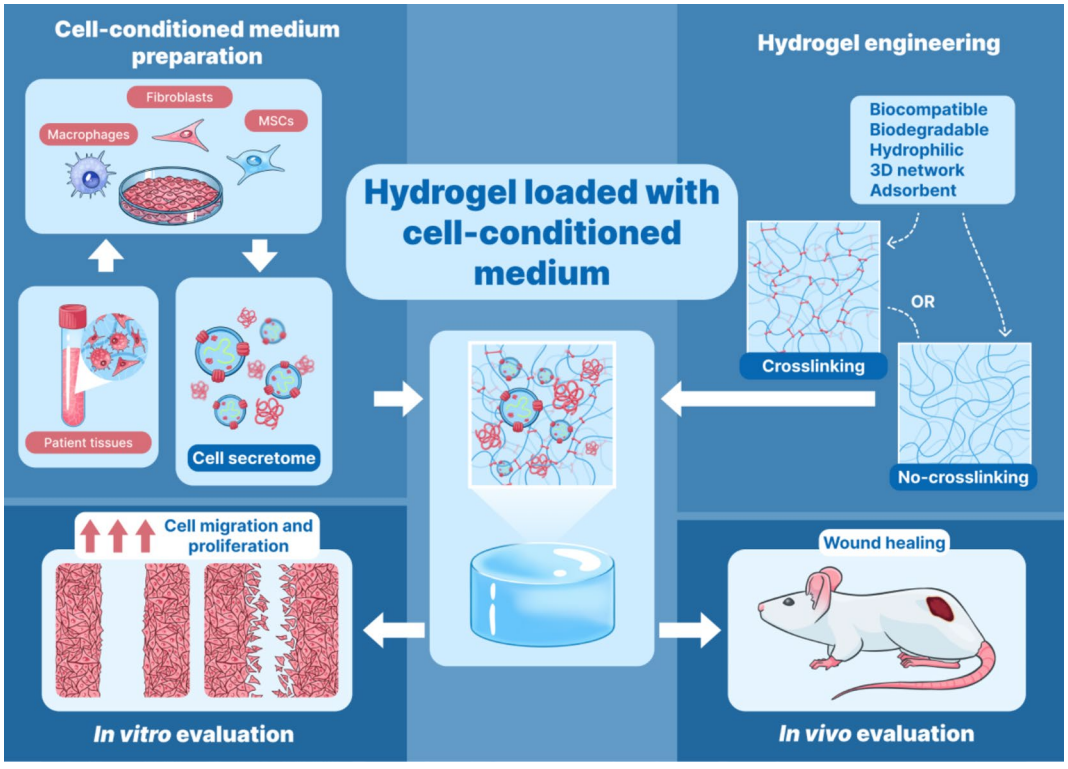

Fig. 1 The key stages of fabrication and preclinical studies of hydrogel-based dressings loaded with cell-conditioned medium intended for wound healing applications

Eligibility criteria

The identified articles were selected using the inclusion and exclusion criteria. The inclusion criteria included the following limitations: (1) stem cells secretome (non-cellular components); (2) hydrogel; (3) in vivo experiments (preclinical and/or clinical trials); (4) skin damage (wounds, burns, ulcers, etc.); (5) topical application; (6) English language; (7) 2019–2024 years of publishing. The exclusion criteria were as follows: (1) reviews, editorials, letters, books, conference papers and abstracts; (2) duplicates; (3) insufficient data. After selecting the appropriate studies based on the inclusion and exclusion criteria, a final list of articles was analyzed in a qualitative manner.

To assure the quality of the selection process the PICO elements were exploited. In this review, the types of participants included all animal varieties/types irrespective of the species, sex and age. Furthermore, the included studies must have used full-thickness skin defect models (wounds and burns). The interventions analyzed represented studies that used a hydrogel matrix with the stem cell secretome as a wound dressing. These were the primary criteria for studies to be included. Studies with no hydrogel matrix or no stem cell secretome were excluded. As types of control studies with a blank control, those on the wound treatment without a hydrogel matrix and/or secretome as the control were selected to the review. Studies that analyzed the wound contraction efficiency as a wound size difference before and after treatment were included to analyze a pre-defined outcome. Thus, the effectiveness and the wound healing rate of the H-CM-based dressings, compared to hydrogel dressings without CM were evaluated.

Risk of bias and study quality assessment

The assessment of quality for the included studies was performed using the CAMARADES checklist as described elsewhere [48–50]. The evaluation included the following 10 criteria: (1) wound size calculation; (2) random allocation to treatment or control; (3) appropriate control; (4) blinded assessment of outcome; (5) appropriate animal defect model; (6) use of anesthetic on animal model where necessary throughout the study; (7) statement of control of temperature; (8) compliance with animal welfare regulations; (9) peer-reviewed publication; (10) statement of no potential conflict of interests. Each "yes" of the following criteria was given a score = 1, while "no" or "unclear" carried a score = 0. Based on the total score of 10, studies with a score of 0–3 were recognized as high risk studies, those with 4–6 as medium risk studies, and those with 7–10 as studies with a low risk of bias.

The assessment of the bias risk of the included studies was performed using the Robvis tool [51]. The following biases were considered in this evaluation tools: selection bias (random sequence generation, allocation

concealment), detection bias (blinding of participants and outcome assessment), attrition bias (incomplete outcome data), reporting bias (selective outcome reporting), and a bias from other sources.

Data extraction and analysis

The author and year, hydrogel compounds, source of cells, type of skin damage (full-thickness wound, diabetic ulcer, burn), animal model species (mice, rat, sheep), outcomes relevant to wound healing or scar improvement were extracted independently by S.S. and G.N. using a standardized tabular form. The data collection for the descriptive analysis was arranged by using Microsoft Excel 2021 (Microsoft Office, Microsoft Corporation, Redmond, WA, USA) and the Origin Pro version 2018 software (OriginLab Corporation, Northampton, MA, USA). Any difficulties and disagreements encountered during the analysis were resolved by consulting the third author (A.S.).

Results

Study selection and study characteristics

The initial search results included 163 articles: 78 from PubMed and 85 from Scopus. After the removal of 59 duplicates, a total of 104 articles were brought to the screening stage to exclude those that did not meet the eligibility criteria. During the further stage of screening the title and abstract, 52 articles were excluded from the study, since they did not satisfy the inclusion criteria. The remaining 52 articles were subjected to a full-text analysis for the eligibility criteria. As a result of the analysis, 31 articles were found to be ineligible, in particular, 21 of them contained information only on in vitro studies, 2 articles contained only ex vivo experiments, 7 articles did not use a hydrogel matrix, 14 did not use conditioned stem cell medium, and 8 were review articles. Some of the articles contained a combination of the listed ineligibility criteria. Finally, 21 studies were selected for the review. The process of searching and screening the articles is summarized in Fig. 2.

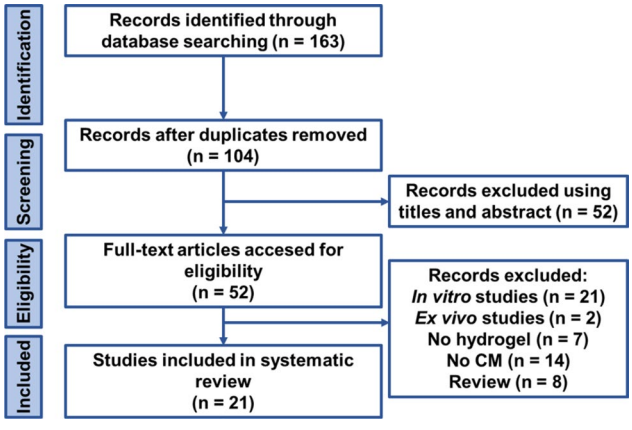

Fig. 2 PRISMA flow diagram representing the selection process of the publications included for the systematic review. *Abbreviations* used, *CM* conditioned medium, *n* number of articles

Further, the articles were categorized for a better understanding of the design and approaches exploited for the fabrication and assessment of regenerating potency of H-CM formulations, involving animal models, and specific wound treatment protocols. Most of the studies represent proof-of-the-concept or concept validation research and describe the hydrogel preparation, CM production and identification of its active components, as well as characterization of the prepared H-CM dressings in vitro and in vivo (Table S1, Supporting Information).

Risk of bias and study quality assessment

According to the result of the CAMARADES quality tool (Table S2, Supporting Information), 19 studies out of 21 (90%) used wound size calculation while assessing the healing efficiency. 8 studies (38%) reported randomization of the experimental and control group allocation. Only 2 included studies (9%) reported the blinded assessment of outcomes. All studies were published in peer-reviewed journals, used appropriate animal models and controls, anesthetized where necessary throughout the study, and stated compliance with the animal welfare regulations. In conclusion, 90% of studies were scored as low risk and 9% were at a medium risk of bias.

According to the Risk of bias (Robvis) tool (Figure S1, Supporting Information), 8 of the 21 studies divided animals into the control and experimental groups randomly and were therefore judged to have a low risk of selection bias. However, none of the articles mentioned that the studies were conducted by assigning, concealing, blinding investigators (unclear risk of bias). Only 2 studies reported blinding of the outcome assessment (low risk of bias). All studies were free from missing data, selective reporting bias, or other biases (low risk of bias). Hence, the quality of the included studies was reliable and acceptable.

Preparing hydrogels loaded with conditioned medium

Hydrogel engineering

The natural and synthetic biocompatible and biodegradable polymers are widely used for hydrogel preparation. During the last five years the classical hydrogel-forming components have been gradually replaced by novel synthetic substances and unusual products of natural origin allowing designing various hydrogel-based delivery systems to be used as wound dressings (Fig. 3).

In detail, 70% of reviewed studies used mainly natural biopolymers or their chemically modified derivatives such as alginate −33% [52–58], chitosan −19% [59], gelatin −14% [60], collagen −14% [61, 62], hyaluronic acid −5% [63], and/or their combinations [64–66]. However,

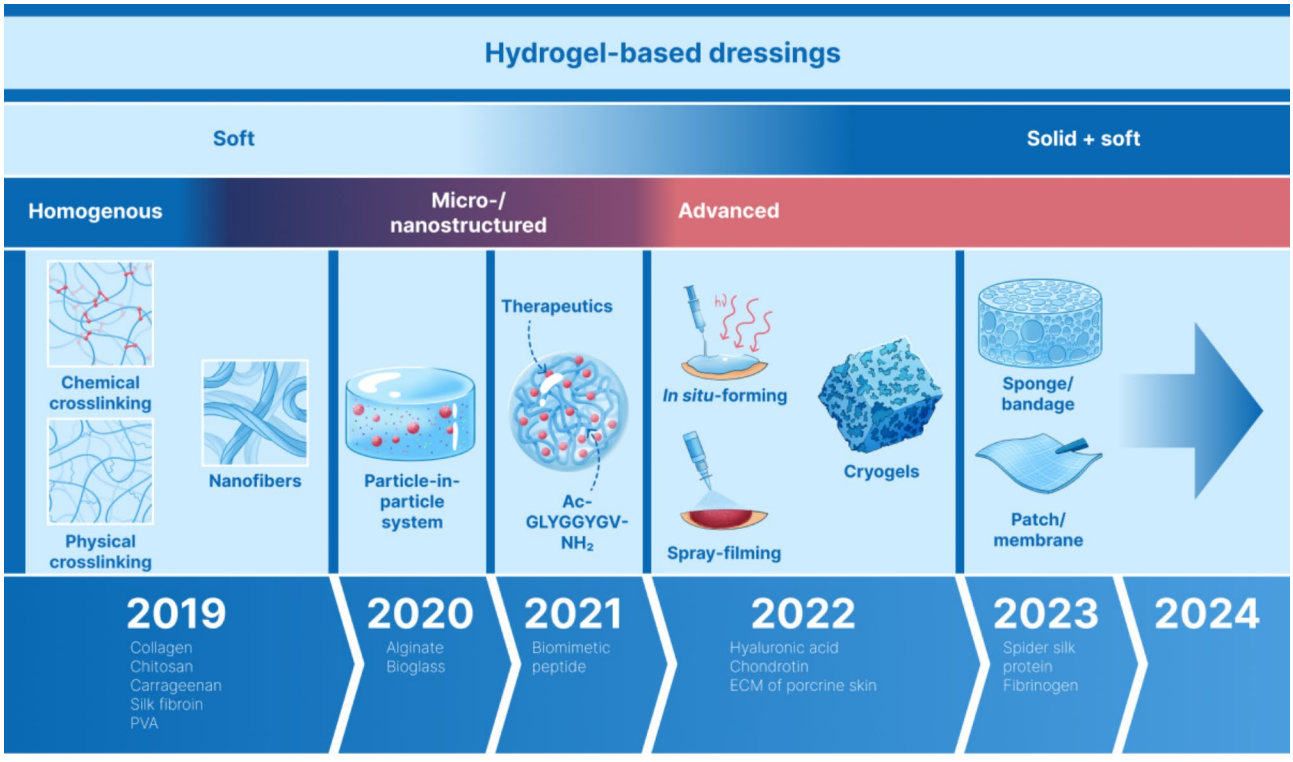

Fig. 3 A five-year retrospective flowchart on the design of wound dressings based on hydrogels loaded with cell-conditioned medium. The panel representing the time point of 2021 is adapted from [52]

other natural biopolymers such as carrageenan [67], fibrinogen [66], and chondroitin [68] were also found in hydrogel formulations. Rare and unique components of natural origin, e.g., silk fibroin [69], spider silk fusion protein [70], decellularized extracellular matrix (ECM) of porcine skin [71], synthetic polymers like cellulose or its modifications [72], poly(vinyl alcohol) [67], short bio-inspired octapeptide [52] or bioceramic materials (e.g., bioglass) [57] were introduced to design hydrogel-based dressings. Within the selection analyzed, the final hydrogels represented mainly soft delivery systems [55, 57, 59, 61, 63–65, 70–72], or solid bandages [53], sponges [56, 62], membranes [58], or films [54, 66].

The hydrogel structure represents a three-dimensional network which acts as a hydrophilic matrix ensuring prolonged and continuous release of embedded proteins used for tissue regeneration (Table 1). The hydrogel structure is usually homogeneous, but some studies have developed nano-, microstructure-bearing composites, e.g., by using silk fibroin nanofibers [69], or by encapsulating CM components such as extracellular vesicles (exosomes) [56]. Alternatively, multilayer constructs were engineered using the particle-in-particle approach, e.g., alginate microparticles doped with proteins stimulating wound healing, and drug-containing poly(lactic-co-glycolic) acid (PLGA) microspheres to sequentially deliver bioactive molecules [57].

Hydrogels containing CM are commonly prepared in their final "ready-to-use" form, however advanced formulations such as in situ-forming grafted hyaluronic acid hydrogels suggest simultaneous crosslinking and gelation directly at the site of application [63]. To prepare a stable hydrogel matrix, their chemical modification or physical treatment is performed. Calcium-based ionic crosslinking in alginate hydrogels [53–55, 57, 65] dominates over photopolymerization [60, 63], temperature-induced [64, 69–71], freeze-thaw [67], solvent-induced gelation [52] or covalent crosslinking [62, 68].

Some hydrogels designed were also characterized as microporous materials [52, 53, 60, 68, 70]. The pore diameter was changed by varying the substitution degree and/or concentration of the gel-forming polymer and was shown to affect the release rate of encapsulated proteins of the cell secretome [60, 70]. The mean pore diameter varied greatly from 22 μm to 200 μm. The structure-functional and biopharmaceutical properties such as the protein release kinetics, hydrogel degradation, viscosity and mechanical characteristics of the hydrogels analyzed in the selected articles are shown in Table 1. To enhance the efficiency of the hydrogel treatment, "smart" thermosensitive hydrogels based on chitosan/collagen/β-glycerophosphate hydrogel were also engineered [64]. These matrices were nonfluid at 37 °C and viscous at lower temperatures suggesting a possibility for

Table 1 Design and structure-functional properties of wound dressings loaded with cell-conditioned medium

Delivery system design	Preparation	Hydrogel composition	Mean pore size, μm	Bioactive molecule release kinetics	Mechanical properties	Reference
Soft hydrogel	Photopolymerization of hydrogel components	Gelatin methacrylate, lithiumphenyl-2,4,6-trimethylbenzoyl phosphinate (photoinitiator)	342.3-200.2-180.4	> 75% of protein loaded is released within 10 days	Hydrogel degradation time in PBS at 37 °C varied from 13 to 19 days; tensile strength and viscosity of the hydrogel increased with polymer concentration; the hydrogel was stable within 4–40 °C	[60]
Solid bandage-like dressing	Ionic crosslinking and hydrogel molding followed with subsequent freeze-drying, macrophage seeding or soaking with cell secretome solution	Calcium-crosslinked alginate	122.1 ± 43.6	Burst release in the first 24 h, release of loaded proteins completed within 3 days	Minimal differences in bandage mass were detected during soaking in RPMI	[53]
CM-impregnated dried alg-Ecm patches	Ionic crosslinking and hydrogel molding with subsequent drying with air and impregnation using CM	Calcium-crosslinked mixture of alginate and extracellular matrix of human lung fibroblasts	Homogenous nonporous matrix	Burst release in the first 12 h; steady-state protein quantity released within 3 days	Degradation time of 80% of hydrogel was 7 days; hydrogel is durable at 3 MPa and viscoelastic	[54]
Soft hydrogel	Ionic crosslinking and hydrogel molding	Calcium-crosslinked alginate-gelatin-conditioned medium mixture	Homogenous nonporous matrix	Prolonged release of VEGF within 4 days	Tensile strength was 14.0 ± 0.64 MPa; elongation ratio at break point and Young's modulus were 21.0 ± 2.5 and 2.5 ± 1.2 MPa	[55]
Soft hydrogel	Physical crosslinking due to temperature-induced gelation, molding	Collagen-CM mixture	-	The protein released from the ASP after 24 h (incubation with type I collagenase); most of the ASP was fully digested after 8 h	-	[61]
Soft hydrogel	Physical crosslinking due to temperature-induced gelation	CM - chitosan-collagen- β-glycerophosphate	-	-	Nonfluid gel after incubation at 37 °C; temperature-induced viscosity increase	[64]

Table 1 (continued)

Delivery system design	Preparation	Hydrogel composition	Mean pore size, μm	Bioactive molecule release kinetics	Mechanical properties	Reference
Soft hydrogel	Photo-initiated free-radical crosslinking	Hyaluronic acid-based hydrogel grafted with methacrylic anhydride and N-(2-aminoethyl)-4-[4-(hydroxymethyl)-2-methoxy-5-nitrophenoxy]-butanamide	-	> 60% of protein loaded is released within 16 days	The final modulus increased with the degree of methacryloyl substitution (9182 ± 558 Pa); the ultimate tensile strengths of hydrogel were determined as 86.6 ± 3.1 kPa, 145.4 ± 5.0 kPa, and 103.4 ± 1.5 kPa; the increased crosslinking density caused the hydrogel to become brittle	[63]
Solid sponge-like dressing	Physical crosslinking, molding followed with subsequent freeze-drying	Sodium alginate	Wide mesh structure	Initial burst release, in the first 3 h (about 40% for proteins and 65% for lipids); protein and lipid release plateaued at 32 h	-	[56]
Soft hydrogel	Physical crosslinking	Carboxymethyl cellulose	-	-	-	[72]
Soft micro-structured hydrogel	Particle in particle chemically ionic crosslinking	Soldium alginate/bioglass hydrogel with sodium alginate microparticles loaded with M2 macrophage secretome and PLGA microspheres with encapsulated pirfenidone	-	Sequential release of the encapsulated CM (95% of the cell secretome is released by day 5) and pirfenidone (95% of the encapsulated CM quantity is released by day 20)	Hydrogel was degraded to 80% after 14 days	[57]
Soft hydrogel	Physical crosslinking, solvent-induced gelation	Bioinspired octapeptide, GV8 (Ac-GLYGGYGV-NH2); cell secretome	10; 33	> 50% of secretome release at days 2–3	-	[52]
Soft hydrogel	Ionic crosslinking and hydrogel molding	Calcium-crosslinked alginate-gelatin-CM mixture	-	-	-	[65]
Solid sponge-like dressing	Ionic crosslinking, molding followed with subsequent freeze-drying	Genipin crosslinked collagen, CM	-	-	-	[62]
Soft hydrogel	Physical crosslinking, temperature-induced gelation	Decellularized extracellular matrix (ECM) of porcine skin, CM	-	-	-	[71]

Table 1 (continued)

Delivery system design	Preparation	Hydrogel composition	Mean pore size, μm	Bioactive molecule release kinetics	Mechanical properties	Reference
Soft hydrogel	Physical crosslinking, temperature-induced gelation	Chitosan; medium from rat bone marrow MMSC	-	-	-	[59]
Soft nanostructured hydrogel	Physical crosslinking, temperature-induced gelation	Silk fibroin self-assembled nanofibers, concentrated CM	-	TGF-β1, IGFBP-1, and PDGF-AB are release within 9 days	Viscosity increased with nanofiber concentration in hydrogel; CM addition decrease hydrogel viscosity	[69]
Soft hydrogel	Physical crosslinking, cryo-gelation	Suckerin-silk fusion proteins, CM	4–70; 42–206 (in case of a freeze-thawed hydrogel)	The cell secretome released by the day 18	Viscoelastic, with a higher shear storage modulus than the loss modulus; with 90% of degradation occurring on days 13 and 18	[70]
Soft hydrogel patch	Physical and chemical crosslinking	Fibrinogen, chitosan, CM	3–5	EGF and KGF were released rapidly during a week, and then maintained a relatively stable and slow-releasing effect for up to 28 days	The Young's modulus of elasticity in tension was 5.5 ± 1.2 MPa and tensile fracture amplitude was 44.6 ± 6.5%	[66]
Soft hydrogel	Physical crosslinking, temperature-induced gelation	PVA, carageenan, CM	-	-	-	[67]
Soft hydrogel patch	Ionic molding and crosslinking, punching	Calcium-crosslinked alginate	-	-	-	[58]
Soft hydrogel	Polymer dissolution and double enzymatic and covalent crosslinking	Aldehyde-based chondroitin sulfate-dopamine-carboxymethyl chitosan	Length 131.4 ± 23.3; width 75.8 ± 5.0	-	High plasticity; 13 s of the gelation time; withstands large elastic deformation; re-assembles after being damaged to form a complete hydrogel due to the natural dynamic; tensile strength, which is 0.72 MPa; completely degraded by day 10	[68]

more effective filling of various types of wounds, including severe burns [64].

Isolation and proteome profiling of cell-derived conditioned medium

In recent decades, numerous studies have demonstrated the beneficial effects of the cell secretome on wound healing [52, 54–56, 59, 64, 66–69, 71, 72], and the number of articles on this topic continues to grow rapidly.

According to the selection analyzed, primary cultures and/or cultures from biobanks or commercially available collections are used for the CM preparation. More than 50% of the selected articles used mesenchymal stem/stromal cells (MSCs) as the secretome sources. Although MSCs are considered to have low immunogenicity [73, 74], recently, there have been a growing number of articles demonstrating that MSCs do not have a full immunological privilege in an immunocompetent allogeneic host [75–77]. Therefore, the review also considers other sources of CM including the following animal and human cell types: murine macrophages, in particular RAW 264.7 cells [53, 57], human M2 macrophages derived from monocytes THP-1 [58], dermal fibroblasts [62, 70] and human keratinocytes HaCaT [70], and human embryonic kidney (HEK) 293 cells [65].

The CM production is performed in the lab-scale quantities and based on cell culturing under predetermined conditions using supplemented cell culture media, which may contain additional components to promote cell polarization or growth factors [53, 60, 61]. Prior to the secretome harvesting, an antibiotic component is usually removed from the culture medium. Further, the purification of the obtained medium using centrifugation or filtration is performed to eliminate undesired cell debris. Afterward, the samples are concentrated with a molecular weight cut-off (MWCO) filter. Then, cell CM is prepared for long-term manipulations and storage by freezing at -20 °C – -80 °C or freeze-drying [59, 60, 63, 65, 67, 69, 70]. However, during cell culturing some unusual conditions can be exploited to enrich the medium with cellular factors and bioactive molecules. For example, hypoxic atmosphere [60], gamma-irradiation [78], or transfected cells overexpressing antioxidant proteins (nuclear factor erythroid 2–related factor 2) [65] were used. The typical cell lines, their key characteristics and specific cultivation parameters to prepare cell CM are presented in Table 2. The resultant cell CM product is characterized by a large diversity of its composition, although the proteome profiling and detailed identification of its composition has been performed in several studies [53, 54, 59, 60, 69]. The most representative groups of biologically active molecules detected were growth factors, cytokines, chemokines and the others, including the ECM components (Fig. 4).

Encapsulation of conditioned medium into a hydrogel matrix

To incorporate CM into a hydrogel network, the prepared secretome product was directly mixed with hydrogel precursors or a preliminary prepared hydrogel and allowed for gelation and/or mixing at pre-determined time and temperature conditions [52, 55, 60–65, 67, 68, 70–72]. In several studies, crosslinking or photopolymerization were performed after obtaining the H-CM mixture [60]. In the case of solid dressings, the dry fabricated patches or bandages were impregnated with a CM solution [53, 54, 66]. To produce sponge-like H-CM dressings, CM was initially introduced into a sodium alginate solution that was subsequently molded and freeze-dried [56]. In the case of micro-/nanostructured systems, CM was firstly encapsulated into sodium alginate microparticles that were later embedded in the hydrogel matrix [57] or directly encapsulated into nanofiber hydrogels [69].

In vitro studies of hydrogels loaded with cell-conditioned medium

To evaluate the biocompatibility and cell proliferative activity of H-CM formulations, a wide range of methods were used, as presented in Table 3. Thus, the wound scratch was the most popular test for assessing the rate of cell migration imitating the wound healing process [52, 54, 58, 60, 69, 70].

To assess the proliferative activity, the CCK8 method with staining of living/ dead cells was used [57, 63, 64, 68, 69]. The articles considered also other crucial processes that occurred in cells during wound healing, such as collagen deposition [54, 58], tube formation [60, 63], cell migration [54, 63], changes in cell phenotype [57, 63], fibroblast differentiation [69], oxidative stress [65], inflammation and immune response [57, 61]. In general, all methods showed good biocompatibility and low cytotoxicity with a remarkable cell survival and proliferation for the hydrogels and H-CM formulations (Fig. 5).

In vivo wound healing potency and efficacy of hydrogels loaded with cell-conditioned medium as wound dressings

Models of wound defects in animals

Wounds represent disruptions in the integrity of the cutaneous barrier caused by surgery, trauma, or burns. Based on the statistical study, only in 2014 acute wounds resulted in 17.2 million hospital visits and this trend seems to gradually increase [80].

To explore the efficacy of novel wound healing tools and proposed strategies, animal models are actively exploited. To replicate the wound healing process, the majority of reviewed studies used small animals (mice, rats). Around 66% of the articles presented experiments on mice. Among them, 57% used a full-thickness cutaneous wound model, 36% reproduced diabetic ulcers, and

Table 2 Cell lines and culture parameters to produce cell-conditioned medium

Cell origin	Tissue	Cell type, morphology	Cell line type	Specific culture conditions	Passage number	Reference
Human	Adipose tissue	Mesenchymal stem cells	Primary cells, home-made	Hypoxia (37 °C, 1% oxygen and 5% CO_2 for 48 h)	P4 - P6	[60]
Murine (male C57BL/6 or mRFP1 mice)	Bone marrow	Monocytes	Primary cells, home-made	Monocyte polarization to M0 (no additives), and M1, M2a, M2c macrophage due to cytokine (LPS, IFN-g, IL-4 13, IL-13, IL-10) addition during 24 h	-	[53]
Human	Bone marrow	Mesenchymal stem cells	Self-renewing cells; PT-2501, Lonza	-	-	[54]
Human	Umbilical cord	Mesenchymal stem cells	Transformed cells, primary cells	The cells were transfected to produce hCAP-18/LL-37	P4-P6	[55]
Human	Redundant skin tissue samples from abdominoplasty or face-lift surgery	Dermal fibroblasts	Primary cells	-	P3	[61]
Human	Umbilical cord	Mesenchymal stem cells	Primary cells	-	Several P cycles	[64]
Human	Placentas from parturients after cesarean section	Clusters of cells comprising amnion	Primary cells	-	P0	[63]
Human	Adipose tissues	Mesenchymal stem cells	Primary cells	-	P3	[56]
Human	Placentas from parturient after cesarean section	Mesenchymal stem cells	Primary cells	Hypoxia (1% oxygen)	P1	[72]
Murine	Tumor in a male mouse induced with the Abelson murine leukemia virus	Monocyte/ macrophage	Transformed cells, RAW 264.7 from the cell bank of Chinese Academy of Sciences Typical Culture Preservation Committee	Bioglass ion extracts (1/128) added to the culture medium to polarize monocytes to M2-macrophages	-	[57]
Human	Adipose tissue	Mesenchymal stem cells	Primary cells	-	P 6–8	[52]
Human	Kidney of a human embryo	Epithelial cells	Transformed cells; HEK293, the National Cell Bank of Iran	The cells were transfected with pcDNA3.1-NRF2 plasmid	P5, P15, P20	[65]
Sheep	Skin biopsy	Dermal fibroblast; Ovine epidermal keratinocytes	Primary cells	Fibroblasts and keratinocytes were initially co-cultured to obtain highly pure both cell types	P3	[62]
Human	Adipose tissue	Stromal cells	Primary cells	-	P3-P6	[71]
Human	Placenta tissue	Multipotent mesenchymal stromal cells	Primary cells	-	P3	[59]
Human	Umbilical cords	Mesenchymal stem cells	Primary cells	-	P3-P6	[69]
Human	Blood	Mononuclear cells	Primary cells	Cells were treated by γ-irradiation (2 × 30 Gy) to induce apoptosis/ necroptosis	-	[78, 94]
Rat	Nasal mucosa	Ecto-mesenchymal stem cells	Primary cells	-	-	[66]
Human	Adipose tissue	Mesenchymal stem cells	Transformed cells; hTERT immortalized SCRC-4000), ATCC	-	P6-P10	[70]
Human	Skin	Multipotent stromal cells	Primary cells	The cells were tested to check viability and phenotypic changes before and after cultures, remaining viable and phenotypically unchanged during the assays	-	[67]

Table 2 (continued)

Cell origin	Tissue	Cell type, morphology	Cell line type	Specific culture conditions	Passage number	Reference
Human	Peripheral blood from an acute monocytic leukemia patient	Monocyte/ macrophage	Transformed cells, THP-1, ATCC	Monocyte polarization to M0, M1, M2-macrophages adding PMA, LPS, IFN-g, IL-4 and IL-13	-	[58]

one article (about 7%) focused on the healing of third-degree burns. The second most popular animal model was a rat model (29%). Among the rat model studies, the distribution was as follows: 83% - full-thickness wound, 17% (one article) - II-IIIa-degree burns infected with *Staphylococcus aureus*. Only one study using big animals (sheep) with a full-thickness skin wound model was found [62].

An in vivo full-thickness acute wound model is the most common one in this review, but other types of wound models, including burns [59, 64] or skin flaps [71] are also considered (Table 4). To reproduce an acute wound, the animals were anesthetized, and full-thickness skin wounds were created on their backs. A biopsy punch, surgical scissors or pre-heated molds (in the case of burn modelling) were applied. The existing wound models varied by their mean size (from 5.8 mm to 14.9 mm) and geometry (Table 4). To avoid the *panniculus carnosus* muscle contraction, a splitting ring tightly sutured to the skin around the wound by 4/0 suture was utilized [55, 65].

Within the selected articles, two studies dealing with difficult-to-heal burn wounds were analyzed. Rodents such as mice and rats were used in these protocols. In detail, mice were anesthetized, and an iron mold heated to 95 °C was placed on the hairless back for 10 s to generate a burn with a square wound area (1.5 cm^2). Wounds were debrided by removing necrotic tissue with sterile tweezers and washing with an aqueous solution of 3% hydrogen peroxide. Then, using a sterile cotton swab, the injured skin was covered with H-CM dressing, which was changed twice a day. In the other study, burns were created by applying a rectangular metal box with a square bottom filled with pre-heated paraffin to the shaved back skin of anesthetized rats for 30 s. The resultant wound area was 4 cm^2. 12 h after the formation of the burn wound, it was infected with *Staphylococcus aureus* as the pathogenic flora [59].

In the majority of the selected studies, wound models have been created in healthy animals. However, it is known that in related chronic diseases, in particular, in diabetes, wound healing is not sufficient and in some cases is accompanied by complications. A wound model in a diabetic animal is also often used and presented in selected articles [53, 57, 63, 70, 72]. For example, wounds were induced in 10–12-week-old male C57BL/KsJ db/db mice with leptin receptor deficient diabetes, having the blood glucose level higher than 300 mg/dL [63]. Another model included diabetes associated with hyperglycemia (glucose level of 300 mg/dl), induced in 5-week- or 8-week-old mice by a single intraperitoneal injection of streptozotocin (180 mg/kg – 200 mg/kg) [57, 72]. To produce diabetes in 6-week-old C57BL/6 wild type mice, a liver disease progression aggravation diet and a normal

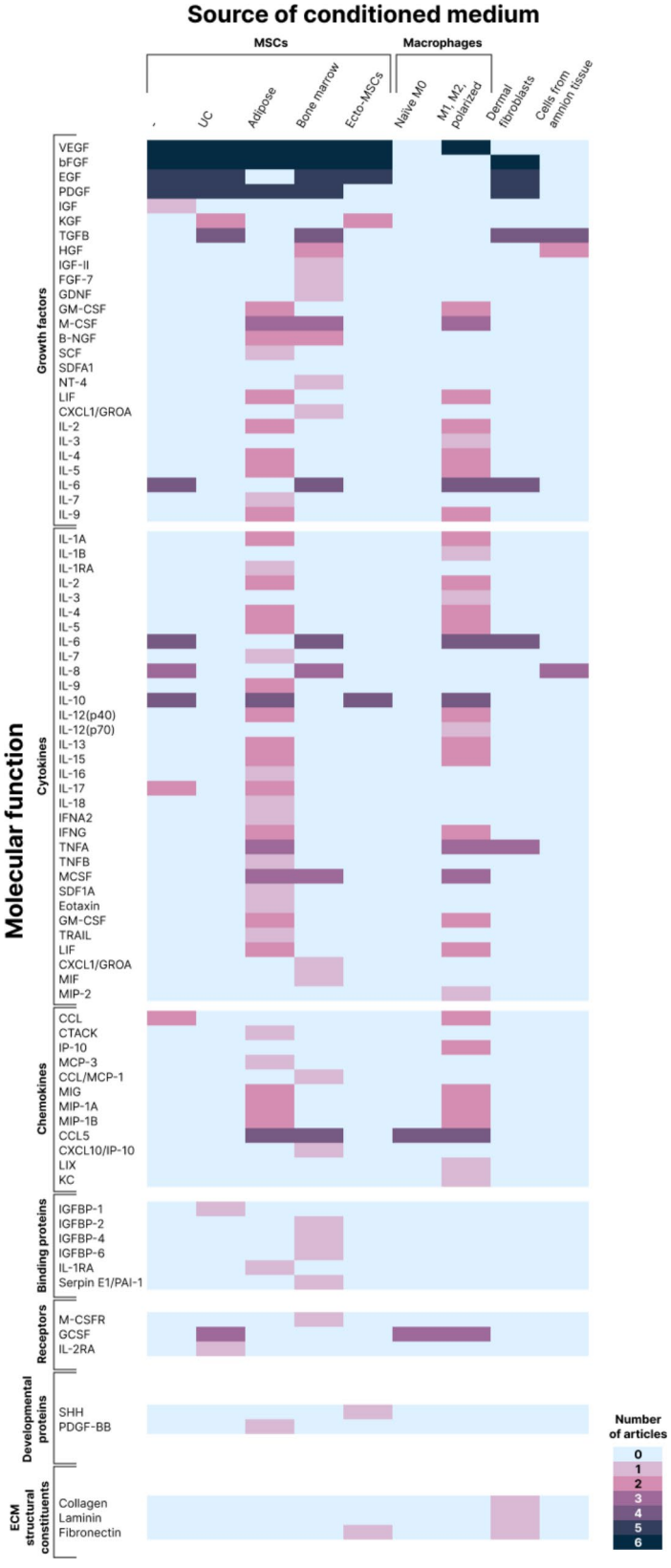

Fig. 4 (See legend on next page.)

(See figure on previous page.)

Fig. 4 The major components of the proteomic profiles of the cell-conditioned media produced and analyzed within the selected articles. The molecules are scored by the incidence of their detection in the analyzed selection [53–55, 60, 61, 63–66, 69, 79]. The molecular function of the proteins is presented according to the classification from the UniProt database. *Abbreviations VEGF* Vascular endothelial growth factor, *bFGF* Basic fibroblast growth factor, *EGF* Epidermal growth factor, *PDGF* Platelet-derived growth factor, *IGF* Insulin-like growth factor, *KGF* Keratinocyte growth factor, *TGFB* Transforming growth factor beta, *HGF* Hepatocyte growth factor, *IGF-II* Insulin-like growth factor 2, *FGF-7* Fibroblast growth factor 7, *GDNF* Glial cell line-derived neurotrophic factor, *GM-CSF* Granulocyte-macrophage colony-stimulating factor, *M-CSF* Macrophage colony-stimulating factor, *B-NGF* Beta-nerve growth factor, *SCF* Stem cell factor, *SDF-1alpha* Stromal cell-derived factor 1, *NT-4* Neurotrophin-4, *LIF* Leukemia inhibitory factor, *CXCL1/GROalpha* Growth-related oncogene-alpha, *IL-2* Interleukin-2, *IL-3* Interleukin-3, *IL-4* Interleukin-4, *IL-5* Interleukin-5, *IL-6* Interleukin-6, *IL-7* Interleukin-7, *IL-8* Interleukin-8, *IL-9* Interleukin-9, *IL-1alpha* Interleukin-1 alpha, *IL-1beta* Interleukin-1 beta, *IL-1ra* Interleukin-1 receptor antagonist, *IL-10* Interleukin-10, *IL-12(p40)* Interleukin-12 subunit beta, *IL-12(p70)* Interleukin-12 heterodimer, *IL-13* Interleukin-13, *IL-15* Interleukin-15, *IL-16* Interleukin-16, *IL-17* Interleukin-17, *IL-18* Interleukin-18, *IFN-alpha2* Interferon alpha-2, *IFN-gamma* Interferon gamma, *TNF-alpha* Tumor necrosis factor alpha, *TNF-beta* Tumor necrosis factor beta, *TRAIL* Tumor necrosis factor-related apoptosis-inducing ligand, *MIF* Migration inhibitory factor, *MIP-2* Macrophage inflammatory protein-2, *CCL* C-C motif chemokine ligand, *CTACK* Cutaneous T-cell-attracting chemokine, *MCP-3* Monocyte-chemotactic protein 3, *CCL/MCP-1* Monocyte chemoattractant protein-1, *MIG* Monokine induced gamma interferon, *MIP-1alpha* Macrophage inflammatory protein-1 alpha, *MIP-1beta* Macrophage inflammatory protein-1 beta, *CCL5* C-C motif chemokine ligand 5, *CXCL10/IP-10* Interferon gamma-induced protein 10, *LIX* LPS-induced CXC chemokine, *KC* Keratinocyte-derived chemokine, *IGFBP-1* Insulin-like growth factor-binding protein-1, *IGFBP-2* Insulin-like growth factor-binding protein-2, *IGFBP-4* Insulin-like growth factor-binding protein-4, *IGFBP-6* Insulin-like growth factor-binding protein-6, *Serpin E1/PAI-1* Endothelial plasminogen activator inhibitor/ Plasminogen activator inhibitor-1, *M-CSF R* Recombinant macrophage colony-stimulating factor, G-*CSF* Granulocyte colony-stimulating factor, *IL-2Ralpha* Interleukin-2 receptor alpha, *SHH* Sonic hedgehog chemokine, *PDGF-BB* Platelet-derived growth factor-BB homodimer, *UC* Umbilical cord: *MSCs* Mesenchymal stem/stromal cells

chow diet were applied for 2 weeks. Then, the blood glucose of both groups was measured and compared to determine the onset of diabetes [70].

Wound healing protocols

H-CM formulations have been investigated as wound dressings in animal models using different protocols (Table 4). Most commonly, the efficacy of dressings was evaluated over a time-course of 7, 14 or 21 days. Sterile formulations were applied once to the wound defect area immediately after the surgery using a sterile transparent barrier (e.g., Tegaderm®), an antibiotic-impregnated gauze or alternative tools to cover the wound and to protect the hydrogels once installed [52–56, 61, 62, 67, 69, 70, 72]. At the same time, the patches were sutured to skin around the wound or, after the hydrogel application, the skin flap was replaced onto the wound site and sutured with nylon to the wound edges [66, 71]. However, in one of studies the experimental protocol assumed that the hydrogel containing NRF2-CM should be deposited on the wound only after injecting MSCs [65]. In several studies, the wound dressing was changed once, daily or at 2–3 day intervals during the given time-course. In the case of advanced *in situ* formation or spray-filming hydrogels, the treatment involved photopolymerization and hydrogel-spraying stages, respectively [63, 68].

The animals were divided into experimental and control groups including positive and negative controls respectively. Then, they were anesthetized and full-thickness skin wounds were created on their backs. After the treatment, the regions corresponding to the created wounds were analyzed in each group. The wound closure was monitored in the time-course, which also included several intermediate time points to control the wound contraction on days 0, 2, 4, 7 and 14 or 28 [54, 56, 61, 66].

Wound healing efficiency

To estimate the wound healing efficiency of H-CM, the wound area was examined within a certain interval to assess the wound closure rate macroscopically and/or by means of the histological analysis and immunohistochemistry staining [52–72]. Besides, the following parameters were monitored: abilities of cells to proliferate [71], migrate, and form tubes [67]; neovascularization and new vessel maturation [52, 54–56, 65, 68, 69, 72]; epidermis thickness [62]; keratinocyte migration and maturation [55, 58, 70]; collagen deposition and density [56–60]; epithelialization [55–57, 59, 61, 62, 65, 68, 72]; fibroblast migration [55]; granulation tissue formation [56, 61, 64, 67]; angiogenesis [54, 55, 60, 63, 67, 70]; inflammatory cell (macrophage) infiltration [58, 59, 63–65, 67, 71, 72] and expression levels of inflammation-related genes [53, 72]. Additionally, PCR-based estimation of cytokine or chemokine expression [72] or LC-MS/MS analysis of wound proteome was conducted [56]. Proliferation and migration of endothelial cells, collagen deposition, neovascularization, angiogenesis, and keratinocyte maturation were observed in the case of all H-CM formulations. The engineered dressings were demonstrated to decrease the inflammatory response [72] and to modulate macrophage polarization to the M2-phenotype [57, 60, 63]. The molecular mechanisms of wound healing due to application of cell secretome-containing hydrogels included Akt/mTOR and MAPK signaling pathway, downregulating the expression levels of proinflammatory agents such as IL-1β, IL-6, CXCL-1, and CXCL-2, as well as expression of proteins involved in wound healing (e.g., Fga, Fgg, F13a1, Tnc, Arg1, Anxa5, Col1a1, Dcn, EGFR, VEGF, HGF, IGF and etc.) [56, 60, 67, 72]. The regenerated tissues were characterized by the expression of CD31, a vascular differentiation marker [53, 54, 57, 60, 70], Ki-67, a cell proliferation marker [53, 64, 71], α-SMA indicating the mature vessel-like structure [53, 54, 58, 69], P63, a

Table 3 Methods for evaluating in vitro biocompatibility and cell proliferative activity of hydrogels loaded with cell conditioned medium using model cell lines

Method	Model cell line	Parameters	Outcomes	Reference
Wound scratch assay	Human umbilical vein endothelial cells	The migration rate is measured as the difference of the width in between cell monolayer parts at predetermined time points	Enhanced cell migration and faster wound closure	[60]
	Human skin fibroblasts			[54]
	Fibroblasts or human umbilical vein endothelial cells			[69]
	Human dermal fibroblast			[58]
	Immortalized human HaCaT keratinocytes			[70]
				[52]
Cell proliferation assay	Human mesenchymal stromal cells	Cell Counting Kit-8 assay	Good biocompatibility, low cytotoxicity, clearly supported cell survival and proliferation	[64]
	Human umbilical vein endothelial cells			[63]
	RAW 264.7 murine-derived macrophages			[57]
	Human fibroblasts and human umbilical vein endothelial cells			[69]
	L929 murine fibroblasts			[68]
Collagen deposition assay	Human skin fibroblasts	Quantitative analysis of immunofluorescence staining collagen type I	Promoted collagen synthesis	[54]
	Human dermal fibroblasts			[58]
Tube formation assay	Human umbilical vein endothelial cells	Quantitative microscopic analysis of loop number	Promoted tube formation	[60]
				[63]
Cell migration assay	Human epidermal CB-HK-001 keratinocytes	Transwell membrane assay (8 mm pore size)	Induced cell migration	[54]
	Human umbilical vein endothelial cells			[63]
Phenotype change analysis	Murine bone marrow macrophages	Quantitative real-time PCR of total RNA (GAPDH, CD206, CCR7 genes)	Upregulated expression of the M2 macrophage marker CD206, reduced expression of the M1 macrophage marker CCR7	[63]
	RAW 264.7 murine-derived macrophages	Expression of macrophage markers, including induced nitric oxide synthase (iNOS, M1), and arginase (ARG, M2) by flow cytometry	Stimulation of M2-polarization of macrophages	[57]
Fibroblast differentiation assay	Human fibroblasts	α-SMA mRNA expression	Downregulation of α-SMA expression; inhibition of proliferation fibroblasts into myofibroblasts leading to scarless healing	[69]
Inflammation gene expression	RAW 264.7 murine-derived macrophages	Quantitative real-time PCR of total RNA	Supression of pro-inflammation gene IL-23 expression and upregulation of anti-inflammation gene IL-10	[57]
Immune response	Human peripheral blood mononuclear cells	Cell proliferative response due to incorporation of tritiated thymidine (3 H-TdR) and its DNA binding is analyzed	No significant difference in PBMC proliferation (no immune response)	[61]
Cell viability	Human dermal fibroblasts	MTT assay	No cytotoxic effect, increased cell proliferation	[55]
Assessment of cytoprotectivity against H_2O_2 toxicity	Human mesenchymal stromal cells	MTT assay, additional treatments of the cells with 250 μM H_2O_2 solution for 24 h to induce cell death	Significant reduction in cell death caused by H_2O_2	[65]

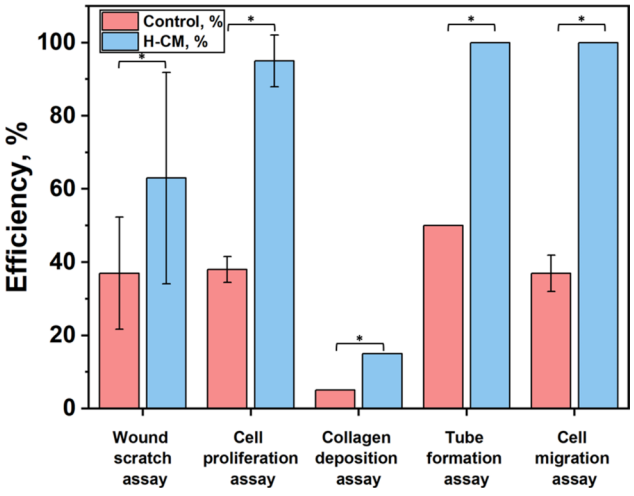

Fig. 5 Representative image of the main in vitro methods assessing effectiveness on cell proliferation, cell migration, tube formation and collagen deposition of hydrogels loaded with conditioned medium. The data were normalized using percent relative abundance. The control bar represents the data collected in the case of samples that did not contain conditioned medium. The data is shown as mean ± standard deviation; $*p < 0.05$, according to two sample *t*-test. *Abbreviations* used, *H-CM* hydrogel loaded with cell-conditioned medium

unique marker of the epidermal stem cells [66], collagen I, collagen III [57] and cytokeratins [58], whereas CD206 expression in the treated tissues indicated the presence of M2-macrophages [58, 63]. The cellular-molecular response induced by each developed formulation is summarized in Table S3, Supporting Information.

Despite the variety of the techniques used, the visual monitoring of wound contraction remains one of the most important evaluations to determine the efficiency of the treatment applied. The remaining wound area at a specific time point was quantitatively calculated to assess the wound closure rate as a percentage of the wound region normalized to that of day 0, using an image processing software [54]. The main factors for assessing the effectiveness of wound healing are its size and healing time. The healing time was described as the time required for the complete reepithelialization of the wound [64–66, 71]. In the majority of studies the wound contraction rate was investigated by taking photographs and adjusting them to a standard scale, using an image processing software. The analysis of the selected articles has demonstrated that H-CM effectively promoted regeneration in acute and chronic wounds (Fig. 6). H-CM dressings showed the highest efficiency of wound contraction in both healthy and diabetic groups, especially in the early stages (6–8 days). These results are consistent with the in vitro experiments showing the increased proliferative and angiogenesis activity of H-CM formulations.

Almost all the articles we found describe the positive outcomes from applying H-CM onto the skin injury area. The most frequently observed effects involved: enhanced cellular activity of dermal fibroblasts and endothelial cells, significantly accelerated wound contraction and promoted wound healing, reduced inflammation with no fibrotic scar formation, and enhanced re-epithelialization and angiogenesis.

Discussion

Hydrogels have demonstrated a great potential as dressings for the treatment of skin injuries [81–85], and for tissue or 3D scaffold engineering [86, 87]. Their final state can be tuned depending on the desired application. A variety of soft and solid hydrogel-based dressings have been developed during the last five years. Cell-derived CM has been added to hydrogel formulations, thus combining a hydrogel matrix and the cell secretome to enhance skin regeneration capacity and wound healing [42, 53, 60, 88]. Hydrogels are simple to prepare, and their mechanical properties, skin adhesion, porosity, rheological characteristics, and release kinetics can be easily adapted and controlled [88, 89]. Cell-CM represents a large ensemble of proteins of different molecular weights (from 5 to 504 kDa) and molecular functions [90], as well as exosomes [91]. These are mainly hydrophilic and readily encapsulated into a hydrogel network during cross-linking or polymerization. To tackle the prolonged and/or controlled release of proteins, micro-/nanostructured systems can be designed [56, 57].

However, scaling up the production of a hydrogel is challenging, especially using such components as the ECM. These components have a great composition variability, which may cause difficulties in the standardization of the technology and the final product. Moreover, it was found that ECM hydrogels loaded with ASC-derived CM did not influence wound healing in a skin flap rat model as compared to the control groups [71]. It may be explained by several reasons. First, the therapeutic effect is influenced by the CM dosage in the hydrogel. We suggest that this limitation may have taken place, since the CM concentration used in that study was as small as one-eighteenth of the volume. It is likely that this amount may not have been sufficient to produce a clear therapeutic effect, especially considering that most of the studies presented in this review used one-to-one ratios of CM and a hydrogel by volume. Second, the retention of the ECM hydrogel remained unclear. It was hard to distinguish the ECM hydrogel and native donor collagen fibers microscopically in the histological samples. Moreover, the release of growth factors could not be measured in the in vivo model. Third, an important limitation was rather rapid wound healing in the control group of rats, which may affect the beneficial influence of H-CM. The authors suggested that it might be more relevant to use rats with defective wound healing (e.g., diabetic animals) or larger

Table 4 Research protocols for assessing the hydrogels loaded with cell-conditioned medium in animal models of wound management

Animal model	Animal age, strain, health status	Wound type and size	Wounds/animal	Number of animals	Target groups	Control groups	Time course, including intermediate control points	Dressing change	Notes	Reference
Murine	20-month-old, C57BL/6J, healthy	Acute (full-thickness), diameter 10 mm	1	12	1) GelMA + F12 group ($n = 6$); 2) GelMA + hypo-CM ($n = 6$); 3) GelMA + nor-CM ($n = 6$)	1) Blank ($n = 6$); 2) GelMA ($n = 6$)	0, 4, 8 and 12 days	-		[60]
	4–5-month-old, C57BL/6, healthy	Acute (full-thickness excisional), diameter 6 mm	1	60	1) CG hydrogel-embedded with CM ($n = 10$); 2) PVA hydrogel-embedded with CM ($n = 11$)	1) No treatment ($n = 12$); 2) CG hydrogel ($n = 9$); 3) PVA hydrogel ($n = 10$); 4) CM ($n = 8$)	3 and 14 days	-		[67]
	8-week-old, C57BL/6, diabetic	Acute, diameter 10 mm	1	45	1) SA/BG-SA-PLGA ($n = 9$); 2) SA/BGSA-PLGAPFD ($n = 9$); 3) SA/BG-SACM-PLGA ($n = 9$); 4) SA/BG-SACM-PLGAPFD ($n = 9$)	1) No treatment ($n = 9$)	6, 12, and 18 days	-		[57]
	10-week-old, C57/BL6, healthy	Acute (full-thickness), diameter 5 mm	1	NA	1) GV8 peptide hydrogel containing CM (n = NA)	1) No treatment (n = NA); 2) GV8 peptide hydrogel (n = NA)	0, 2, 5 and 7 days	-		[52]
	6-week-old, C57BL/6, healthy	Acute (burn), square wound area (with a side-length of 15 mm)	1	72	1) CM-hydrogel ($n = 18$)	1) uCM ($n = 18$); 2) CM ($n = 18$)	4, 14, and 28 days	Twice per day		[64]
	6-week-old, C57BL/6 wild-type, diabetic	Acute (full-thickness splinting), diameter 6 mm	4	14	1) Secretome-laden fusion hydrogel (n = NA)	1) PBS (n = NA); 2) Secretome (n = NA); 3) Fusion hydrogel (n = NA)	0, 2, 4, 6, 8 and 10 days	-		[70]
	10-12-week-old, C57BL/KsJ db/db, diabetic	Acute (full thickness), diameter 8 mm	2	18	1) CM-gel ($n = 6$)	1) Gel ($n = 6$); 2) Vaseline gauze ($n = 6$)	0, 7 and 12 days	-		[63]
	C57, healthy	Acute (full-thickness), diameter 10 mm	1	NA	1) CM-containing hydrogel (0,5%, n = NA); 2) CM-containing hydrogel (1%, n = NA); 3) CM-containing hydrogel (2%, n = NA)	1) No treatment (n = NA)	7,14 and 21 days	-		[69]
	16-week-old, db/db, diabetic	Acute (full-thickness), diameter 6 mm	2	NA	1) CM0-containing bandage ($n = 5–7$); 2) CM1-containing bandage ($n = 5–7$); 3) CM2a-containing bandage ($n = 5–7$); 4) CM2c-containing bandage ($n = 5–7$)	1) Control bandage ($n = 5–7$)	0, 3, 5, 7 and 10 days	-		[53]

Table 4 (continued)

Animal model	Animal age, strain, health status	Wound type and size	Wounds/animal	Number of animals	Target groups	Control groups	Time course, including intermediate control points	Dressing change	Notes	Reference
	6-week-old, BALB/c, healthy	Acute (full-thickness), diameter 8 mm	2	12	1) AC (*n* = 3); 2) AEC (*n* = 3)	1) AS (*n* = 3); 2) AES (*n* = 3)	0, 2, 4, 7 and 14 days	-		[54]
	6-week-old, BALB/c, healthy	Acute (full-thickness), diameter 8 mm	2	24	1) M2-CCM (*n* = 3); 2) M2-hFDM-CCM (*n* = 3)	1) Serum-free media (negative control, *n* = 3); 2) 10%FBS-supplemented media (positive control, *n* = 3)	0,7, and 14 days	Every 2–3 days		[58]
	2-month-old, BALB/c, healthy	Acute (full-thickness), diameter 10 mm	1	NA	1) Collagen hydrogel containing 200 μg/mL DFCM-KM1 (n = NA); 2) Collagen hydrogel containing 400 μg/mL DFCM-KM (n = NA); 3) Collagen hydrogel containing 400 μg/mL DFCM-FM (n = NA); 4) Collagen hydrogel containing 800 μg/mL DFCM-FM(n = NA)	1) No treatment (*n* = 6); 2) Collagen hydrogel (*n* = 6)	0, 7, 14, and 17 days	Twice (at day 0 and at day 7)		[61]
	21-week-old, strain is not indicated, healthy	Acute (full-thickness), diameter 6 mm	2	NA	1) Lyo-secretome-loaded alginate dressing (n = NA)	2) Alginate dressing (n = NA)	3, 7, 14, and 21 days	-		[56]
	5-week-old, ICR, diabetic	Acute (full-thickness), diameter 8 mm	2	NA	1) Hydrogel containing normoxic CM (n = NA); 2) Hydrogel containing hypoxic CM (n = NA)	1) Hydrogel containing standard medium (n = NA)	0, 1, 3, 5, 7, and 9 days	-		[72]

Table 4 (continued)

Animal model	Animal age, strain, health status	Wound type and size	Wounds/animal	Number of animals	Target groups	Control groups	Time course, including intermediate control points	Dressing change	Notes	Reference
Rat	Adult, Sprague-Dawley, healthy	Acute (circular, full-thickness), diameter 10 mm	1	36	1) Hydrogel containing CM ($n=9$)	1) Saline solution ($n=9$); 2) CM ($n=9$); 3) Hydrogel ($n=9$)	0, 3, 7, 10 and 14 days	-		[68]
	Adult, Sprague-Dawley, healthy	Acute (full-thickess), diameter 15 mm	3	20	1)Bioactive functional composite patches contained EMSCs-CM (n = NA)	1) No treatment (n = NA); 2) Composite patches without EMSCs-CM (n = NA)	14, 21, d 28 days	-		[66]
	Wistar, healthy	Acute (full-thickness), diameter 20 mm	1	36	1) SA/G-V-CM group ($n=3$); 2) SA/G-LL-37-CM ($n=3$)	1) PBS ($n=3$); 2) SA/G-PBS ($n=3$)	0,7,14 and 21 days	-		[55]
	Wistar, healthy	Acute (full-thickness), diameter 20 mm	1	36	1) Hydrogel loaded with NRF2-CM and combined with MSCs ($n=3$); 2) Hydrogel loaded with V-CM and combined with MSCs ($n=3$)	1) PBS ($n=3$); 2) MSCs ($n=3$)	0,7,14 and 21 days	-		[65]
	8-week-old, Wistar, healthy	Pedicled skin flap	1	60	1) ECM hydrogel with CMe ($n=5$)	1) DMEM ($n=5$); 2) ECM hydrogel ($n=5$); 3) CMe ($n=5$)	7,14, and 28 days	-		[71]
	3-month-old, Wistar, healthy	Acute (burn), area of 4 cm^2	1	40	1) MMSC secretome-based chitosan gel ($n=10$)	1) Control (medical Vaseline oil, $n=10$); 2) Bepanthen Plus (cream for external use, $n=10$); 3) Miramistin solution for topical application 0.01%, $n=10$	4 and 7 days	The formulations were applied 24 h later and then daily for 3 days ($n=5$) or 7 days ($n=5$) in each group	Wound area contaminated with *Staphylococcus aureus*	[59]
Sheep	6-8-month-old, Siamese long tail, healthy	Acute (full-thickness), area 20cm^2	4	6	1) Collagen hydrogel loaded with DFCM ($n=6$); 2) Collagen sponge scaffold with freshly harvested skin cell ($n=6$); 3) Platelet-rich-plasma gel ($n=6$)	1) No treatment ($n=6$)	0, 7, 14 and 21 days	Thrice, in 7 day interval		[62]

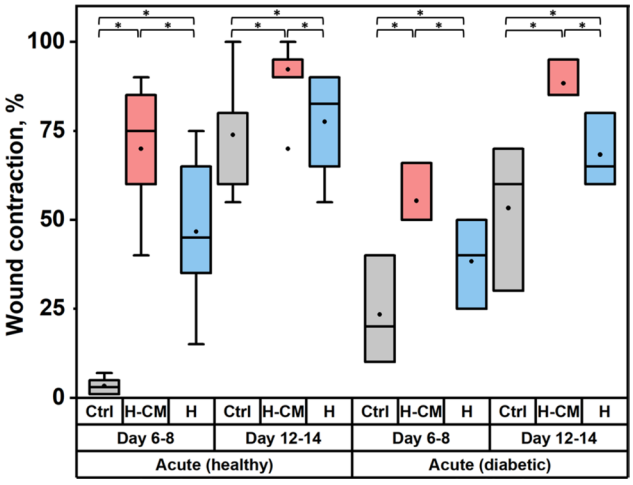

Fig. 6 The quantitative analysis of wound contraction rate in vivo. The data represent healthy and diabetic animal models with relative healing effectiveness in control and target (treated with hydrogel and hydrogel loaded with cell-conditioned medium) groups after 6–8 and 12–14 days of wounding. The data is shown as mean ± standard deviation; $*p < 0.1$, according to one-way ANOVA test. *Abbreviations* used, *Ctrl* control, *H-CM* hydrogel loaded with cell-conditioned medium, *H* hydrogel

mammals such as pigs, which are more similar to humans in regard to wound healing.

Other important limitations are related to the cell CM therapeutics that lacks standardization of bioprocessing, and information on its composition and stability. For instance, the MSC secretome is characterized by the potential difference in its composition depending on the type, origin and localization of donor cells from which the secretome was obtained. This systematic review presents CM produced by primary cultures obtained from the waste fat of patients who had undergone liposuction [60, 71], from mice and human bone marrow [53, 54], from the umbilical cord of newborn infants delivered by caesarean sections [55, 59, 63, 64, 69, 72], from skin tissue samples after abdominoplasty or face-lift surgery [56, 61], from nasal septum and inferior nasal concha of rats [66]. Other sources of CM included cell lines cultivated or purchased from commercial companies such as RAW 264.7 cells (a murine-derived macrophage cell line), L929 cells (an areolar-derived fibroblast cell line), hTERT immortalized adipose-derived mesenchymal stem cells (ADMSC, SCRC-4000, (American type culture collection (ATCC)) [52], stable HEK-293 cell line expressing NRF2 (NRF2-HEK-293) [65], human telomerase reverse transcriptase (hTERT)–immortalized ADMSCs (SCRC-4000) [70], THP-1, human monocyte-like cells (ATCC) [58]. We propose that such a large variation in cell sources and their potential differences in secretomes imposes certain difficulties on the process of standardizing the composition of a therapeutic product used in the wound treatment. The secretome contains >>300 of proteins with different activity [92] (according to LC-MS/MS data of CM profiling [67, 70, 93]), and it seems quite difficult to analyze the target effect of each of them on tissue regeneration. Therefore, the regeneration and wound healing capacity is explained by synergy of all CM components. However, the existing research on the development of hydrogels for their use as wound dressings is still represented by numerous proof-of-concept studies. It is interesting to note that, within the last five years, there have been no studies describing the ongoing clinical trials of the H-CM dressings. Only one paper mentioned the start of the MARSYAS II trials involving a total of 132 patients, assessing the efficiency of the APOSEC secretome-based treatment, but this study is in progress and has not yet been completed [78, 94].

To further implement hydrogel-based dressings and efficiently translate them into clinics, the manufacturing technology should be optimized to result in the GMP-compliant and "ready-off-the shelf" final product [56]. The technique used should meet the sterility requirements. In particular, the possibility applying the modern approaches such as 3D bioprinting or electrospinning should be explored in the future. These techniques may represent promising alternatives to already existing hydrogel production strategies requiring multiple stages [95–97]. To analyze the CM's wound healing properties after the incorporation into a hydrogel matrix, a greater number of studies should be conducted with the focus on disease-specific skin injuries (diabetic wounds, ulcers, and burns), involving complete *in vitro/in vivo* evaluation. For this purpose, modern microfluidic wound-on-a-chip or healing-on-a-chip models can be exploited [98–100]. Moreover, to reduce the laboratory costs associated with in vivo studies, alternative ex vivo wound models are being developed [101–103], and the possibility of the use of other small animal models, e.g., leech, and specific conditions for wound healing are still being discussed [104].

Conclusions

The development of hydrogel-based dressings for the treatment of skin defects and wounds is a dynamic area, with hundreds of publications. This multidisciplinary research field involves chemical engineering, regenerative medicine and biotechnology. In this review, we provide a systematic analysis of the key points on the design, structural-functional properties, and *in vitro/in vivo* assessment of H-CM dressings for the wound treatment. The cell secretome embedded into hydrogel matrices is an effective tool to heal skin lesions and wounds. In the future, more studies exploring novel approaches for H-CM fabrication, or harmonized protocols for animal studies are likely to be published. We also expect further translation of the designed dressings into

clinical research to validate the efficiency and safety of the designed regenerative technology.

Abbreviations

3D	Three-dimensional
ADMSC	Adipose-derived mesenchymal stem cells
Alg-Ecm	Alginate- extracellular matrix
ANOVA	Analysis of variance
APOSEC	Secretome of apoptotic peripheral blood cells
ASP	Acellular skin patch
ASC	Adipose stromal cell
CM	Conditioned medium
CCK8	Cell Counting Kit-8
ECM	Extracellular matrix
H-CM	Hydrogel loaded with conditioned medium
hTERT	Human telomerase reverse transcriptase
LC MS/MS	Liquid chromatography–mass spectrometry
MARSYAS	Marshall system for aerospace system simulation
MSCs	Mesenchymal stem/ stromal cells
MWCO	Molecular weight cut-off
NRF2	Nuclear factor erythroid 2-related factor 2
PCR	Polymerase chain reaction
PLGA	Poly (lactic-co-glycolic acid)
RPMI	Roswell Park Memorial Institute
PVA	Polyvinyl alcohol

Supplementary Information

The online version contains supplementary material available at https://doi.org/10.1186/s13287-024-03976-x.

Supplementary Material 1

Acknowledgements

We thank Svetlana Kotova for her critical reading of the manuscript and technical assistance.

Author contributions

Conceptualization was performed by S.S., G.N., O.S., A.S.; methodology by S.S., G.N.; article screening and formal analysis S.S., G.N., A.S.; funding acquisition by A.S.; supervision by A.S., P.T.; project management by S.S., G.N., Y.K., A.S., P.T.; writing – original draft by S.S., G.N., Y.K., O.S.; writing-review & editing by M.V., A.S., P.T. All authors read and approved the final manuscript.

Funding

The part of the study devoted to hydrogel engineering, its loading with therapeutics and functional assessment was supported by the Russian Science Foundation, grant № 24-45-10012. The part of the study related to the analysis of tissue regeneration efficiency was funded by the Russian Science Foundation, grant № 23-15-00481.

Data availability

The datasets used and/or analyzed during the current study are available from the corresponding author on reasonable request.

Declarations

Ethics approval and consent to participate

Not applicable.

Consent for publication

Not applicable.

Competing interests

The authors declare that they have no competing interests.

Author details

[1]Institute for Regenerative Medicine, Sechenov University, 8-2 Trubetskaya St, Moscow 119991, Russia
[2]Department of Regenerative Medicine, Cell Science Research Center, Royan Institute for Stem Cell Biology and Technology, Academic Center for Education, Culture and Research, Tehran 1665666311, Iran
[3]World-Class Research Center "Digital Biodesign and Personalized Healthcare", Sechenov University, 8-2 Trubetskaya St, Moscow 119991, Russia

Received: 6 August 2024 / Accepted: 4 October 2024
Published online: 17 October 2024

References

1. Peltier S, Adib Y, Nicosia L, Ly Ka So S, Da Silva C, Serror K, et al. *In vitro* effects of wound-dressings on key wound healing properties of dermal fibroblasts. Exp Dermatol. 2024;33:e15098.
2. Safoine M, Paquette C, Gingras G-M, Fradette J. Improving cutaneous wound healing in diabetic mice using naturally derived tissue-engineered biological dressings produced under serum-free conditions. Stem Cells Int. 2024;1:3601101.
3. Thormann U, Marti S, Lensmith E, Lanz M, Herzig S, Naef R, et al. Formulation and dermal delivery of a new active pharmaceutical ingredient in an *in vitro* wound model for the treatment of chronic ulcers. Eur J Pharm Biopharm. 2024;202:114373.
4. Li Y, Chen S, Zhang M, Ma X, Zhao J, Ji Y. Novel injectable, self-healing, long-effective bacteriostatic, and healed-promoting hydrogel wound dressing and controlled drug delivery mechanisms. ACS Appl Mater Interfaces. 2024;16:2140–53.
5. Zhang Q-Y, Tan J, Nie R, Song Y-T, Zhou X-L, Feng Z-Y, et al. Acceleration of wound healing by composite small intestinal submucosa hydrogels through immunomodulation. Compos Part B Eng. 2023;254:110550.
6. Byun H, Han Y, Kim E, Jun I, Lee J, Jeong H, et al. Cell-homing and immunomodulatory composite hydrogels for effective wound healing with neovascularization. Bioact Mater. 2024;36:185–202.
7. Li X, Chen X, Guan L, He W, Yin W, Ye D, et al. Bioactive metal ion-coordinated dynamic hydrogel with antibacterial, immunomodulatory, and angiogenic activities for infected wound repair. ACS Appl Mater Interfaces. 2024;16:32104–17.
8. Pereira RVS, EzEldeen M, Ugarte-Berzal E, Martens E, Malengier-Devlies B, Vandooren J, et al. Physiological fibrin hydrogel modulates immune cells and molecules and accelerates mouse skin wound healing. Front Immunol. 2023;14:1170153.
9. Zhou L, Liu F, You J, Zhou B, Guo W, Qu W, et al. A novel self-pumping Janus dressing for promoting wound immunomodulation and diabetic wound healing. Adv Healthc Mater. 2024;13:2303460.
10. Ghelich P, Samandari M, Hassani Najafabadi A, Tanguay A, Quint J, Menon N, et al. Dissolvable immunomodulatory microneedles for treatment of skin wounds. Adv Healthc Mater. 2024;13:2302836.
11. Petrova VA, Poshina DN, Golovkin AS, Mishanin AI, Zhuravskii SG, Yukina GY, et al. Electrospun composites of chitosan with cerium oxide nanoparticles for wound healing applications: characterization and biocompatibility evaluation *in vitro* and *in vivo*. Polymers. 2024;16:1787.
12. Paolella G, Montefusco A, Caputo I, Gorrasi G, Viscusi G. Quercetin encapsulated polycaprolactone-polyvinylpyrrolidone electrospun membranes as a delivery system for wound healing applications. Eur J Pharm Biopharm. 2024;200:114314.
13. Hautmann A, Hedtke T, Sislema-Muñoz S, Martins-Schalinski J, Schmelzer CEH, Groth T. Design of a composite wound dressing: combining an electrospun fleece with a free-standing multilayer film. Mater. 2024;2:100060.
14. Cheng K, Deng Y, Qiu L, Song S, Chen L, Wang L, et al. Heparin-loaded hierarchical fiber/microsphere scaffolds for anti-inflammatory and promoting wound healing. Smart Mater Med. 2024;5:240–50.
15. Girard F, Lajoye C, Camman M, Tissot N, Berthelot Pedurand F, Tandon B, et al. First advanced bilayer scaffolds for tailored skin tissue engineering produced via electrospinning and melt electrowriting. Adv Funct Mater. 2024;34:2314757.
16. Amante C, Neagu M, Falcone G, Russo P, Aquino RP, Nicolais L, et al. Hyaluronate loaded advanced wound dressing in form of *in situ* forming hydrogel

powders: Formulation, characterization, and therapeutic potential. Int J Biol Macromol. 2024;274:133192.
17. Peng X, Peng Q, Wu M, Wang W, Gao Y, Liu X, et al. A pH and temperature dual-responsive microgel-embedded, adhesive, and tough hydrogel for drug delivery and wound healing. ACS Appl Mater Interfaces. 2023;15:19560–73.
18. Chambre L, Rosselle L, Barras A, Aydin D, Loczechin A, Gunbay S, et al. Photothermally active cryogel devices for effective release of antimicrobial peptides: on-demand treatment of infections. ACS Appl Mater Interfaces. 2020;12:56805–14.
19. Conzatti G, Nadal C, Berthelot J, Vachoud L, Labour M-N, Tourrette A, et al. Chitosan-PNIPAM thermogel associated with hydrogel microspheres as a smart formulation for MSC injection. ACS Appl Bio Mater. 2024;7:3033–40.
20. Balitaan JNI, Hsiao C-D, Yeh J-M, Santiago KS. Innovation inspired by nature: biocompatible self-healing injectable hydrogels based on modified-β-chitin for wound healing. Int J Biol Macromol. 2020;162:723–36.
21. Chen B, Wu S, Ye Q. Fabrication and characterization of biodegradable KH560 crosslinked chitin hydrogels with high toughness and good biocompatibility. Carbohydr Polym. 2021;259:117707.
22. Mao L, Hu S, Gao Y, Wang L, Zhao W, Fu L, et al. Biodegradable and electroactive regenerated bacterial cellulose/MXene ($Ti_3C_2T_x$) composite hydrogel as wound dressing for accelerating skin wound healing under electrical stimulation. Adv Healthc Mater. 2020;9:2000872.
23. Ren W, Sands M, Han X, Tsipursky M, Irudayaraj J. Hydrogel-based oxygen and drug delivery dressing for improved wound healing. ACS Omega. 2024;9:24095–104.
24. Dong X, Sun Q, Xu J, Wang T. Development of a multifunctional composite hydrogel for enhanced wound healing: Hemostasis, sterilization, and long-term moisturizing properties. ACS Appl Mater Interfaces. 2024;16:2972–83.
25. Hua Y, Wang K, Huo Y, Zhuang Y, Wang Y, Fang W, et al. Four-dimensional hydrogel dressing adaptable to the urethral microenvironment for scarless urethral reconstruction. Nat Commun. 2023;14:7632.
26. Arno MC, Inam M, Weems AC, Li Z, Binch ALA, Platt CI, et al. Exploiting the role of nanoparticle shape in enhancing hydrogel adhesive and mechanical properties. Nat Commun. 2020;11:1420.
27. Teoh JH, Mozhi A, Sunil V, Tay SM, Fuh J, Wang C-H. 3D printing personalized, photocrosslinkable hydrogel wound dressings for the treatment of thermal burns. Adv Funct Mater. 2021;31:2105932.
28. García-Fernández L, Olmeda-Lozano M, Benito-Garzón L, Pérez-Caballer A, San Román J, Vázquez-Lasa B. Injectable hydrogel-based drug delivery system for cartilage regeneration. Mater Sci Eng C. 2020;110:110702.
29. del Andrade J, Pérez-Álvarez L, Sáez-Martínez V, Benito-Cid S, Ruiz-Rubio L, Pérez-González R, et al. Wound healing and antibacterial chitosan-genipin hydrogels with controlled drug delivery for synergistic anti-inflammatory activity. Int J Biol Macromol. 2022;203:679–94.
30. Ottonelli I, Bighinati A, Adani E, Loll F, Caraffi R, Vandelli MA, et al. Optimization of an injectable hydrogel depot system for the controlled release of retinal-targeted hybrid nanoparticles. Pharmaceutics. 2023;15:25.
31. Pérez-Rafael S, Ivanova K, Stefanov I, Puiggalí J, del Valle LJ, Todorova K, et al. Nanoparticle-driven self-assembling injectable hydrogels provide a multi-factorial approach for chronic wound treatment. Acta Biomater. 2021;134:131–43.
32. Guyot C, Cerruti M, Lerouge S. Injectable, strong and bioadhesive catechol-chitosan hydrogels physically crosslinked using sodium bicarbonate. Mater Sci Eng C. 2021;118:111529.
33. Al Sabbagh C, Seguin J, Agapova E, Kramerich D, Boudy V, Mignet N. Thermosensitive hydrogels for local delivery of 5-fluorouracil as neoadjuvant or adjuvant therapy in colorectal cancer. Eur J Pharm Biopharm. 2020;157:154–64.
34. Xie X, Lei H, Fan D. Antibacterial hydrogel with pH-responsive microcarriers of slow-release VEGF for bacterial infected wounds repair. J Mater Sci Technol. 2023;144:198–212.
35. Gribova V, Petit L, Kocgozlu L, Seguin C, Fournel S, Kichler A, et al. Polyarginine as a simultaneous antimicrobial, immunomodulatory, and miRNA delivery agent within polyanionic hydrogel. Macromol Biosci. 2022;22:2200043.
36. Andretto V, Rosso A, Zilio S, Sidi-Boumedine J, Boschetti G, Sankar S, et al. Peptide-based hydrogel for nanosystems encapsulation: the next generation of localized delivery systems for the treatment of intestinal inflammations. Adv Healthc Mater. 2024;13:2303280.
37. Qian Y, Zheng Y, Jin J, Wu X, Xu K, Dai M, et al. Immunoregulation in diabetic wound repair with a photoenhanced glycyrrhizic acid hydrogel scaffold. Adv Mater. 2022;34:2200521.
38. Fu Y-J, Shi Y-F, Wang L-Y, Zhao Y-F, Wang R-K, Li K, et al. All-natural immunomodulatory bioadhesive hydrogel promotes angiogenesis and diabetic wound healing by regulating macrophage heterogeneity. Adv Sci. 2023;10:2206771.
39. Trujillo S, Gonzalez-Garcia C, Rico P, Reid A, Windmill J, Dalby MJ, et al. Engineered 3D hydrogels with full-length fibronectin that sequester and present growth factors. Biomaterials. 2020;252:120104.
40. Kushibiki T, Mayumi Y, Nakayama E, Azuma R, Ojima K, Horiguchi A, et al. Photocrosslinked gelatin hydrogel improves wound healing and skin flap survival by the sustained release of basic fibroblast growth factor. Sci Rep. 2021;11:23094.
41. Ahangar P, Mills SJ, Smith LE, Strudwick XL, Ting AE, Vaes B, et al. Human multipotent adult progenitor cell-conditioned medium improves wound healing through modulating inflammation and angiogenesis in mice. Stem Cell Res Ther. 2020;11:299.
42. Hodge JG, Decker HE, Robinson JL, Mellott AJ. Tissue-mimetic culture enhances mesenchymal stem cell secretome capacity to improve regenerative activity of keratinocytes and fibroblasts in vitro. Wound Repair Regen. 2023;31:367–83.
43. Kim JH, Green DS, Ju YM, Harrison M, Vaughan JW, Atala A, et al. Identification and characterization of stem cell secretome-based recombinant proteins for wound healing applications. Front Bioeng Biotechnol. 2022;10:954682.
44. Hermann M, Peddi A, Gerhards A, Schmid R, Schmitz D, Arkudas A, et al. Secretome of adipose-derived stem cells cultured in platelet lysate improves migration and viability of keratinocytes. Int J Mol Sci. 2023;24:3522.
45. Silva D, Schirmer L, Pinho TS, Atallah P, Cibrão JR, Lima R, et al. Sustained release of human adipose tissue stem cell secretome from star-shaped poly(ethylene glycol) glycosaminoglycan hydrogels promotes motor improvements after complete transection in spinal cord injury rat model. Adv Healthc Mater. 2023;12:2202803.
46. Page MJ, McKenzie JE, Bossuyt PM, Boutron I, Hoffmann TC, Mulrow CD, et al. The PRISMA 2020 statement: an updated guideline for reporting systematic reviews. BMJ. 2021;372:n71.
47. Moher D, Liberati A, Tetzlaff J, Altman DG, The PRISMA Group. Preferred reporting items for systematic reviews and meta-analyses: the PRISMA statement. Annals Int Med. 2009;151:264–9.
48. Namjoynik A, Islam MA, Islam M. Evaluating the efficacy of human dental pulp stem cells and scaffold combination for bone regeneration in animal models: a systematic review and meta-analysis. Stem Cell Res Ther. 2023;14:132.
49. Huang Q-Y, Zheng H, Shi Q-Y, Xu J-H. Validity of stem cell-loaded scaffolds to facilitate endometrial regeneration and restore fertility: a systematic review and meta-analysis. Front Endocrinol. 2024;15:1397783.
50. Macleod MR, O'Collins T, Howells DW, Donnan GA. Pooling of animal experimental data reveals influence of study design and publication bias. Stroke. 2004;35:1203–8.
51. McGuinness LA, Higgins JPT. Risk-of-bias VISualization (robvis): an R package and Shiny web app for visualizing risk-of-bias assessments. Res Synth Methods. 2021;12:55–61.
52. Hiew SH, Wang JK, Koh K, Yang H, Bacha A, Lin J, et al. Bioinspired short peptide hydrogel for versatile encapsulation and controlled release of growth factor therapeutics. Acta Biomater. 2021;136:111–23.
53. Theocharidis G, Rahmani S, Lee S, Li Z, Lobao A, Kounas K, et al. Murine macrophages or their secretome delivered in alginate dressings enhance impaired wound healing in diabetic mice. Biomaterials. 2022;288:121692.
54. Kwon JW, Savitri C, An B, Yang SW, Park K. Mesenchymal stem cell-derived secretomes-enriched alginate/ extracellular matrix hydrogel patch accelerates skin wound healing. Biomater Res. 2023;27:107.
55. Sabzevari R, Roushandeh AM, Mehdipour A, Alini M, Roudkenar MH. SA/G hydrogel containing hCAP-18/LL-37-engineered WJ-MSCs-derived conditioned medium promoted wound healing in rat model of excision injury. Life Sci. 2020;261:118381.
56. Bari E, Di Silvestre D, Mastracci L, Grillo F, Grisoli P, Marrubini G, et al. GMP-compliant sponge-like dressing containing MSC lyo-secretome: proteomic network of healing in a murine wound model. Eur J Pharm Biopharm. 2020;155:37–48.
57. Ma Z, Song W, He Y, Li H. Multilayer injectable hydrogel system sequentially delivers bioactive substances for each wound healing stage. ACS Appl Mater Interfaces. 2020;12:29787–806.
58. Savitri C, Kwon JW, Drobyshava V, Ha SS, Park K. M2 macrophage-derived concentrated conditioned media significantly improves skin wound healing. Tissue Eng Regen Med. 2022;19:617–28.
59. Kudinov VA, Artyushev RI, Zurina IM, Lapshin RD, Snopova LB, Mukhina IV, et al. Antimicrobial and regenerative effects of placental multipotent

mesenchymal stromal cell secretome-based chitosan gel on infected burns in rats. Pharmaceuticals. 2021;14:1263.
60. Li S, Sun J, Yang J, Yang Y, Ding H, Yu B, et al. Gelatin methacryloyl (GelMA) loaded with concentrated hypoxic pretreated adipose-derived mesenchymal stem cells (ADSCs) conditioned medium promotes wound healing and vascular regeneration in aged skin. Biomater Res. 2023;27:11.
61. Maarof M, Mh Busra MF, Lokanathan Y, Bt Hj Idrus R, Rajab NF, Chowdhury SR. Safety and efficacy of dermal fibroblast conditioned medium (DFCM) fortified collagen hydrogel as acellular 3D skin patch. Drug Deliv Transl Res. 2019;9:144–61.
62. Subramaniam T, Shaiful Hadi N, Sulaiman S, Fauzi MB, Hj Idrus RB, Chowdhury SR, et al. Comparison of three different skin substitutes in promoting wound healing in an ovine model. Burns. 2022;48:1198–208.
63. Zhang Y, Zheng Y, Shu F, Zhou R, Bao B, Xiao S, et al. *In situ*-formed adhesive hyaluronic acid hydrogel with prolonged amnion-derived conditioned medium release for diabetic wound repair. Carbohydr Polym. 2022;276:118752.
64. Zhou P, Li X, Zhang B, Shi Q, Li D, Ju X. A human umbilical cord mesenchymal stem cell-conditioned medium/chitosan/collagen/ β -glycerophosphate thermosensitive hydrogel promotes burn injury healing in mice. BioMed Res Int. 2019;1:5768285.
65. Sabzevari R, Mohammadi Roushandeh A, Alijani -Ghazyani Z, Jahanian-Najafabadi A, Habibi Roudkenar M. SA/G hydrogel containing NRF2-engineered HEK-293-derived CM improves wound healing efficacy of WJ-MSCs in a rat model of excision injury. J Tissue Viability. 2021;30:527–36.
66. Zhang X, Shi W, Wang X, Zou Y, Xiang W, Lu N. Evaluation of the composite skin patch loaded with bioactive functional factors derived from multicellular spheres of EMSCs for regeneration of full-thickness skin defects in rats. Curr Stem Cell Res Ther. 2024;19:1142–52.
67. Robert AW, Azevedo Gomes F, Rode MP, Marques da Silva M, Veleirinho MBDR, Maraschin M, et al. The skin regeneration potential of a pro-angiogenic secretome from human skin-derived multipotent stromal cells. J Tissue Eng. 2019;10:2041731419833391.
68. Wu S, Zhang Z, Xu R, Wei S, Xiong F, Cui W, et al. A spray-filming, tissue-adhesive, and bioactive polysaccharide self-healing hydrogel for skin regeneration. Mater Des. 2022;217:110669.
69. Li M, Zhong L, He W, Ding Z, Hou Q, Zhao Y, et al. Concentrated conditioned medium-loaded silk nanofiber hydrogels with sustained release of bioactive factors to improve skin regeneration. ACS Appl Bio Mater. 2019;2:4397–407.
70. Koh K, Wang JK, Chen JXY, Hiew SH, Cheng HS, Gabryelczyk B, et al. Squid suckerin-spider silk fusion protein hydrogel for delivery of mesenchymal stem cell secretome to chronic wounds. Adv Healthc Mater. 2023;12:2201900.
71. Vriend L, Van Dongen JA, Sinkunas V, Brouwer LA, Buikema HJ, Moreira LF, et al. Limited efficacy of adipose stromal cell secretome-loaded skin-derived hydrogels to augment skin flap regeneration in rats. Stem Cells Dev. 2022;31:630–40.
72. Takahashi H, Ohnishi S, Yamamoto Y, Hayashi T, Murao N, Osawa M, et al. Topical application of conditioned medium from hypoxically cultured amnion-derived mesenchymal stem cells promotes wound healing in diabetic mice. Plast Reconstr Surg. 2021;147:1342.
73. Aguiar Koga BA, Fernandes LA, Fratini P, Sogayar MC, Carreira ACO. Role of MSC-derived small extracellular vesicles in tissue repair and regeneration. Front Cell Dev Biol. 2023;10.
74. Jiang W, Xu J. Immune modulation by mesenchymal stem cells. Cell Prolif. 2020;53:e12712.
75. Chen W, Lv L, Chen N, Cui E. Immunogenicity of mesenchymal stromal/stem cells. Scand J Immunol. 2023;97:e13267.
76. Sanabria-de la Torre R, Quiñones-Vico MI, Fernández-González A, Sánchez-Díaz M, Montero-Vílchez T, Sierra-Sánchez Á, et al. Alloreactive immune response associated to human mesenchymal stromal cells treatment: a systematic review. J Clin Med. 2021;10:2991.
77. Zhou T, Yuan Z, Weng J, Pei D, Du X, He C, et al. Challenges and advances in clinical applications of mesenchymal stromal cells. J Hematol OncolJ Hematol Oncol. 2021;14:24.
78. Gugerell A, Sorgenfrey D, Laggner M, Raimann J, Peterbauer A, Bormann D, et al. Viral safety of APOSECTM: a novel peripheral blood mononuclear cell derived-biological for regenerative medicine. Blood Transfus. 2020;18:30–9.
79. Maarof M, Chowdhury SR, Saim A, Bt Hj Idrus R, Lokanathan Y. Concentration dependent effect of human dermal fibroblast conditioned medium (DFCM) from three various origins on keratinocytes wound healing. Int J Mol Sci. 2020;21:2929.
80. Sen CK. Human wound and its burden: updated 2020 compendium of estimates. Adv Wound Care. 2021;10:281–92.
81. Menassol G, van der Sanden B, Gredy L, Arnol C, Divoux T, Martin DK, et al. Gelatine-collagen photo-crosslinkable 3D matrixes for skin regeneration. Biomater Sci. 2024;12:1738–49.
82. Tricou L-P, Guirguis N, Cherifi K, Matoori S. Zeolite-loaded hydrogels as wound pH-modulating dressings for diabetic wound healing. ACS Appl Bio Mater. 2024.
83. Zhang H, Lu Y, Huang L, Liu P, Ni J, Yang T, et al. Scalable and versatile metal ion solidificated alginate hydrogel for skin wound infection therapy. Adv Healthc Mater. 2024. e2303688.
84. Zhang J, Zhu Y, Zhang Y, Lin W, Ke J, Liu J, et al. A balanced charged hydrogel with anti-biofouling and antioxidant properties for treatment of irradiation-induced skin injury. Mater Sci Eng C Mater Biol Appl. 2021;131:112538.
85. Vila Nova BG, Silva LDS, Andrade M da, de Santana S, da Silva AVS, Sá LCT. The essential oil of Melaleuca Alternifolia incorporated into hydrogel induces antimicrobial and anti-inflammatory effects on infected wounds by *Staphylococcus aureus*. Biomed Pharmacother Biomedecine Pharmacother. 2024;173:116389.
86. Noreen S, Bernkop-Schnürch A. Thiolated poly- and oligosaccharide-based hydrogels for tissue engineering and wound healing. Adv Funct Mater. 2024;34:2310129.
87. Cantoni F, Barbe L, Pohlit H, Tenje M. A perfusable multi-hydrogel vasculature on-chip engineered by 2-photon 3D printing and scaffold molding to improve microfabrication fidelity in hydrogels. Adv Mater Technol. 2024;9:2300718.
88. Doshi RB, Vakil D, Molley TG, Islam MS, Kilian KA, Cunningham C, et al. Mesenchymal stem cell-secretome laden photopolymerizable hydrogels for wound healing. J Biomed Mater Res A. 2024;112:1418–93.
89. Sun Q, Tao S, Bovone G, Han G, Deshmukh D, Tibbitt MW et al. Versatile mechanically tunable hydrogels for therapeutic delivery applications. Adv Healthc Mater. 2024:2304287.
90. Muntiu A, Papait A, Vincenzoni F, Vitali A, Lattanzi W, Romele P, et al. Disclosing the molecular profile of the human amniotic mesenchymal stromal cell secretome by filter-aided sample preparation proteomic characterization. Stem Cell Res Ther. 2023;14:339.
91. Zhou Y, Zhang X-L, Lu S-T, Zhang N-Y, Zhang H-J, Zhang J, et al. Human adipose-derived mesenchymal stem cells-derived exosomes encapsulated in pluronic F127 hydrogel promote wound healing and regeneration. Stem Cell Res Ther. 2022;13:407.
92. Peshkova M, Korneev A, Suleimanov S, Vlasova II, Svistunov A, Kosheleva N, et al. MSCs' conditioned media cytokine and growth factor profiles and their impact on macrophage polarization. Stem Cell Res Ther. 2023;14:142.
93. Bari E, Perteghella S, Di Silvestre D, Sorlini M, Catenacci L, Sorrenti M, et al. Pilot production of mesenchymal stem/stromal freeze-dried secretome for cell-free regenerative nanomedicine: a validated GMP-compliant process. Cells. 2018;7:190.
94. Gugerell A, Gouya-Lechner G, Hofbauer H, Laggner M, Trautinger F, Almer G, et al. Safety and clinical efficacy of the secretome of stressed peripheral blood mononuclear cells in patients with diabetic foot ulcer—study protocol of the randomized, placebo-controlled, double-blind, multicenter, international phase II clinical trial MARSYAS II. Trials. 2021;22:10.
95. Antoshin A, Minaeva E, Koteneva P, Peshkova M, Bikmulina P, Kosheleva N, et al. LIFT of cell spheroids: Proof of concept. Bioprinting. 2023;34:e00297.
96. Khan R, Aslam Khan MU, Stojanović GM, Javed A, Haider S, Abd Razak SI. Fabrication of bilayer nanofibrous-hydrogel scaffold from bacterial cellulose, PVA, and gelatin as advanced dressing for wound healing and soft tissue engineering. ACS Omega. 2024;9:6527–36.
97. Wang X, Wei P, Hu C, Zeng H, Fan Z. 3D printing of Rg3-loaded hydrogel scaffolds: anti-inflammatory and scar-formation related collagen inhibitory effects for scar-free wound healing. J Mater Chem B. 2024;12:4673–85.
98. Biglari S, Le TYL, Tan RP, Wise SG, Zambon A, Codolo G, et al. Simulating inflammation in a wound microenvironment using a dermal wound-on-a-chip model. Adv Healthc Mater. 2019;8:1801307.
99. Zajdel TJ, Shim G, Cohen DJ. Come together: On-chip bioelectric wound closure. Biosens Bioelectron. 2021;192:113479.
100. Shabestani Monfared G, Ertl P, Rothbauer M. An on-chip wound healing assay fabricated by xurography for evaluation of dermal fibroblast cell migration and wound closure. Sci Rep. 2020;10:16192.
101. Lumsden EJ, Kimble RM, Ware RS, Griffin B. Tissue pressure changes and implications on dressing selection when utilising negative pressure wound therapy on an *ex vivo* porcine model. Burns. 2024;50:1241–6.

102. Andersson MÅ, Madsen LB, Schmidtchen A, Puthia M. Development of an experimental *ex vivo* wound model to evaluate antimicrobial efficacy of topical formulations. Int J Mol Sci. 2021;22:5045.
103. Rakita A, Nikolić N, Mildner M, Matiasek J, Elbe-Bürger A. Re-epithelialization and immune cell behaviour *in* an *ex vivo* human skin model. Sci Rep. 2020;10:1.
104. Cialdai F, Colciago A, Pantalone D, Rizzo AM, Zava S, Morbidelli L, et al. Effect of unloading condition on the healing process and effectiveness of platelet rich plasma as a countermeasure: study on *in vivo* and *in vitro* wound healing models. Int J Mol Sci. 2020;21:407.

Publisher's note